

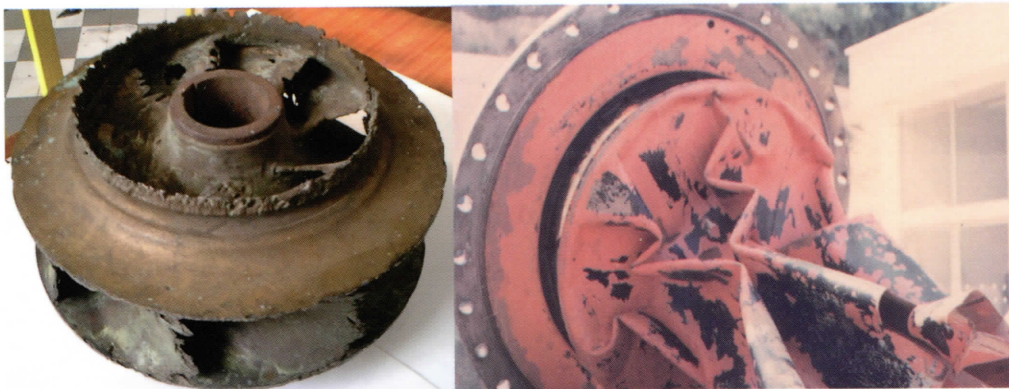


**University of Belgrade, Faculty of Mechanical Engineering,
Belgrade, Serbia, October 26–28, 2011**

**Proceedings of the 4th International Meeting on
CAVITATION AND DYNAMIC PROBLEMS IN HYDRAULIC
MACHINERY AND SYSTEMS**



IAHR-WG2011



Edited by: A. Gajic, M. Benisek, M. Nedeljkovic

A. Gajic
M. Benisek
M. Nedeljkovic

**Proceedings of the 4th International Meeting on
CAVITATION AND DYNAMIC PROBLEMS IN HYDRAULIC
MACHINERY AND SYSTEMS**

Publisher:

University of Belgrade, Faculty of Mechanical Engineering
Kraljice Marije 16,
11120 Belgrade 35, Serbia
Tel: +381.11.3302382
Fax: +381.11.3370364

For publisher:

Dean Prof.Dr.Milorad Milovančević

Editor and Text Coauthor:

Prof.Dr. Aleksandar Obradović

Circulation:

100 copies

Print:

Planeta print
Ruzveltova 10, Belgrade
tel/fax: +381.11.3088129

All rights reserved by Publiser
Unauthorized printing and copying is forbidden

International Advisory Committee

- **Dr A. Ruprecht**, Univ. of Stuttgart, (G) (*president*)
- Prof. F. Avellan, EPFL-LMH, (CH)
- Dr A. Bergant, Litostroj Power, (SI)
- Mr M. Couston, Alstom, (F)
- Prof. E. Egusquiza, Univ. Cataluña, (E)
- Prof. B. Karney, Toronto Univ., (CA)
- Dr H. Keck, Andritz, (CH)
- Mr J. Koutnik, Voith, (G)
- Dr A. Lipej, Turboinstitut, (SI)
- Prof. T. Nielsen, Norwegian Univ. of Sci. & Tech., (N)
- Prof. H. Nilsson, Chalmers Univ., (S)
- Prof. P. Popovski, FME Skopje, (FYROM)
- Prof. R. S. Resiga, Tech. Univ. of Timisoara, (RO)
- Dr A. Skotak, ČKD Blansko Eng, (CZ)
- Prof. H. Tsukamoto, Kyushu Inst. of Tech., (J)
- Prof. Yulin Wu, Tsinghua Univ., (PRC)

National Advisory Committee

- **Academician V. Đorđević**, SANU, (*president*)
- Academician P. Miljanić, SANU
- Academician M. Vukobratović, SANU, AESS
- Prof. M. Dimkić, IJC, Belgrade
- Prof. M. Ivetić, University of Belgrade
- Prof. M. Nedeljković, Min. STD of Serbia
- Prof. N. Rajaković, Min. ME of Serbia
- Mr D. Marković, EPS, Belgrade
- Mr C. Babić, BVK, Belgrade
- Mr V. Pirivatrić, Energoprojekt Co., Belgrade

Organizing Committee

- **Prof. A. Gajić**, FME Belgrade (*president*)
- Prof. M. Benišek, FME, Belgrade
- Prof. S. Čantrak, FME, Belgrade
- Prof. R. Kapor, SDHI, Belgrade
- Prof. M. Milovančević, FME, Belgrade
- Prof. V. Stevanović, FME, Belgrade
- Mr I. Božić, FME, Belgrade
- Mr Dj. Čantrak, FME, Belgrade
- Mr D. Ilić, FME, Belgrade
- Mr B. Ivljanin, FME, Belgrade
- Mr M. Čitaković, HPP »Bajina Bašta«
- Mr D. Stanković, HPP »Iron Gate«
- Mr B. Stišović, Energoprojekt Co., Belgrade

CONTENTS

Session 1: INVITED LECTURES

- H.BREKKE, Historical Review of improved Control Systems by means of the Structure Matrix Method.....1
S. PEJOVIC, Q. F. ZHANG, B. KARNEY, A. GAJIC, Analysis of Pump-Turbine "S" Instability and Reverse Waterhammer Incidents in Hydropower11

Session 2 : HYDRAULIC TRANSIENT

- A. BERGANT, Q. HOU, A. KERAMAT, A. S. TIJESSELING, Experimental and Numerical Analysis of Water Hammer in a Large-Scale PVC Pipeline Apparatus.....27
C.NICOLET, T. KAELBEL, S. ALLIGNE, N. RUCHONNET, P. ALLENBACH, A. BERGANT, F. AVELLAN, Simulation of Water Hammer Induced Column Separation through Electrical Analogy.....37
P. K. DÖRFLER, Pressure wave propagation and damping in a long penstock.....47

Session 3: CAVITATION

- S. CUPILLARD, A.M. GIROUX, R. FRASER, C. DESCHÊNES, Cavitation Modeling in a Propeller Turbine.....67
A. VALLIER, J. REVSTEDT, H. NILSSON, Procedure for the Break-up of Cavitation Sheet.....77
A.KOTENKO, L. NIKOLAYENKO, S. LUGOVA, Development of Cavitation in Torque Flow Pump and Development of Cavitation in Torque Flow Pump87
D. IVANOVIĆ, V. IVANOVIĆ, Effect of Fluid Flow Velocity in the Pipeline to the Appearance Cavitation Spread and its Disappearance After the Pump Drive Failure97

Session 4: SWIRLING FLOW

- A.I. BOSIIOC, C. TANASA, R. S.RESIGA,S. MUNTEAN, Experimental Analysis of Unsteady Velocity in Decelerated Swirling Flows105
S. MUNTEAN, A. BOSIIOC, R. STANCIU, C. TANASA ,R. S.-RESIGA, 3D Numerical Analysis of a Swirling Flow Generator115
A. MÜLLER, S. ALLIGNÉ, F. PARAZ, C. LANDRY, F. AVELLAN, Determination of Hydroacoustic Draft Tube Parameters by High Speed Visualization during Model Testing of a Francis Turbine125
P. RUDOLF, M. JÍZDNÝ, Decomposition of the Swirling Flow Fields133

Session 5: PUMP SYSTEMS

- A. GUSAK, O. DEMCHENKO, I. KAPLUN, A.KOCHEVSKY, Investigation of Small-Sized Axial-Flow Stage of a Borehole Pump for Water Supply143
G. GÍNGA, A. STUPARU, A. BOSIIOC, L. E. ANTON, S. MUNTEAN, 3D Numerical Simulation of the Flow into the Suction Elbow and Impeller of a Storage Pump151
K. TANAKA, T. SATO, A. INOUE, T. NAGAHARA, F. SHIMIZU, M. FUCHIWAKI, Numerical Study of Cavitating flows and Cavitation Surge in a Double-Suction Volute Pump System161
I.MOISÁ, A. STUPARU, R. S.RESIGA, S. MUNTEAN, Inverse Design of a Pump Inducer and Performance Evaluation with 3D Flow Simulation.....171

Session 6: HYDRAULIC OSCILATIONS

- G. OLIMSTAD, B. BØRRESEN T. NIELSEN, Design of a Reversible Pump-Turbine with Purpose to Investigate Stability179
B. HÜBNER, U. SEIDEL, A. D'AGOSTINI NETO, Synchronization and Propagation of Vortex Induced Vibrations in Francis Turbines due to Lock-In Effects based on Coupled Vibro-Acoustic Mode Shapes189
S. ROTH, V. HASMATUCHI, F. BOTERO, M. FARHAT, F. AVELLAN, Influence of the Pump-Turbine Guide Vanes Vibrations on the Pressure Fluctuations in the Rotor-Stator Vaneless Gap199

B. SVINGEN, H. LURAAS, E. C. WALSETH , Frequency Response Measurements and Calculations with Water Column Compensation and Pressure Feedback	213
E. C. WALSETH, B. SVINGEN, T. K. NIELSEN , Investigating the Effect of Turbine Characteristics on the Pressure Response of a System	221
C. LANDRY, S. ALLIGNÉ, V. HASMATUCHI, S. ROTH, A. MUELLER, F. AVELLAN , Non-Linear Stability Analysis of a Reduced Scale Model Pump-Turbine at Off-Design Operation	231

Session 7: FLOW SIMULATION

S. ALLIGNE, C. NICOLET, F. AVELLAN , Identification by CFD Simulation of the Mechanism Inducing Upper Part Load Resonance Phenomenon	241
U. FRATINO, A. PAGANO , Experimental and Numerical Analysis of Perforated Plates	257
P. SEIBERT, M. J. CERVANTES , Runner Cone Separation in Kaplan Turbines	265
J. M. CERVANTES, H. NILSSON , Effects of Rotating Angular-Resolved Inlet Boundary Conditions in the Turbine-99 Kaplan Draft Tube, using OpenFOAM and CFX	273
F. KREY, B. HÜBNER, U. SEIDEL , Transient Simulation of a Pump-Turbine using Coupled Vibro-Acoustic Finite Element Analyses to Investigate Rotor-Stator Interaction Phenomena	279

Session 8: MEASUREMENTS

J. OBROVSKY, B. SEDA, J. ZOUHAR , Experience with Hydraulic Design of Low Specific Speed Turbine	287
B.MULU G., J. M. CERVANTES , Phase-Resolved Velocity Measurements in a Kaplan Draft Tube Model	297
C. TANASA, A. BOSIOC, R. S.RESIGA, S. MUNTEAN , LDV Experimental Measurements of Swirling Flow using Flow-Feedback Jet Injection Method	305
U. KARADŽIĆ, A. BERGANT, P. VUKOSLAVČEVIĆ , Influence of Unsteady Friction on Hydraulic Transients in a High- Head Hydropower plant	313
M. ELTVIK, O. G. DAHLHAUG, H. P. NEOPANE , Prediction of Sediment Erosion in Francis Turbines	321



**4-th International Meeting on
Cavitation and Dynamic Problems in Hydraulic Machinery and Systems,
October, 26-28, 2011, Belgrade, Serbia**

The computational model of the emergence and development of cavitation in torque flow pump

Alexandr Kotenko¹, Lyudmila Nikolayenko¹, Svitlana Lugova²

¹Department of Applied Fluid Dynamics, Sumy State University
Rimskogo-Korsakova str., 2, Sumy, 40007, Ukraine, specialist_pumps@ukr.net, mila_lusia@mail.ru

²Department of Scientific Research, JSC "VNIIAEN"
2-ya Zheleznodorozhnaya str., 2, Sumy, 40003, Ukraine, janeford@rambler.ru

Abstract

We present the results of numerical calculation of velocities and pressure allocation in the flow part (turbine setting) of the torque flow pump type "Turo" in the origin and growth of cavitation using the software ANSYS CFX 11.0. Torque flow pumps yield to centrifugal pumps in terms of efficiency, but also provide reliable and continuous work throughout the period of operation. To estimate the reliability of the pump work it is necessary to focus attention on their cavitation qualities. To ensure in reliable continuous operation of the pumps it is requires to estimate numerically the degree of cavitation growth, as well as features of its origin. To perform the calculation it was constructed the computational domain, which consists of a free camera and the impeller. At the initial stage, we calculated the flow in free of cavitation mode for single-phase medium using a standard k- ϵ turbulence model. In the next step we calculated the model of flow with cavitation. This calculation is performed in a wide range of static pressures at the pump inlet. As a result of the calculation, the areas of origin and growth of cavitation were defined in the flow part of the torque flow pump at different values of NPSH and the cavitation characteristic of the pump was obtained. The results of numerical studies are confirmed by the physical experiments taking place earlier.

Keywords: cavitation, torque flow pump, cavitation curve, numerical calculation, two-phase model.

1. Introduction

Torque flow pumps (TFP) finds an application for the pumping of untreated industrial and domestic waste water, semi finished products in a form of viscous liquids, liquids with solid particles and fibrous inclusions, and various suspensions.

The free chamber (FC) before the impeller (IM) is a constructive feature of the TFP pumps. IM location in the casing cylindrical boring (Fig. 1) and free passage of the fluid main flow through the FC allows the pump to pump mixtures of high concentration of solid impurities without changing the basic parameters and with high cavitation properties

Torque flow pumps yield to centrifugal pumps in efficiency, but they provide reliable and durable work during the entire period of operation.

When assessing the reliability of pumps, special attention is given to cavitation properties. Ability to work without cavitation with increasing the hydraulic resistance at the inlet of the pump makes it possible to increase the concentration of the pumped fluid, and a later demonstration of the cavitation consequences makes it possible to decrease the depth of the foundation laying for pump units. Ultimately, this all leads to increased efficiency of using the TFP pumps [1].

Providing reliable and durable work of pumps requires knowing a quantitative assessment of the cavitation development degree, as well as features of the onset and development of cavitation occurrences.

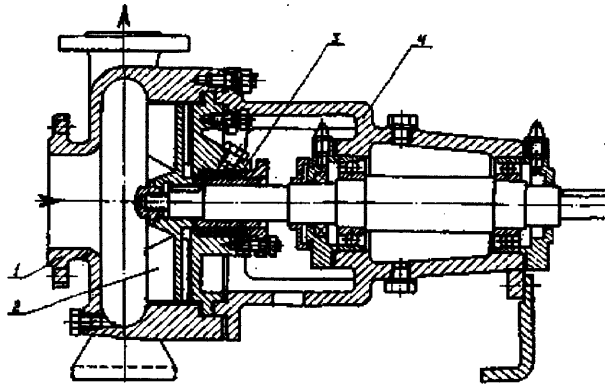


Fig. 1 "Turo" type torque flow pump design (1 – casing; 2 - impeller; 3 – end seal; 4 - bearing housing)

2. Setting numerical investigation of cavitation in the flow path of the torque flow pump

Investigation of cavitation in pumps is conducted mainly on the basis of energy method of research. In this case, cavitation characteristics are built by change of their pressure and power characteristics. The goal of these investigations is to determine a moment when energy parameters on the stalling cavitation characteristic of the pump start to decrease, which indicates the influence of cavitation on the work process in the pump. However, cavitation occurs long before the mentioned characteristics have been changed. It is impossible to determine the time of cavitation occurrence in the pump and to ascertain the location of its onset by using the energy method. Besides, a physical experiment requires high material costs during the investigations.

This paper proposes a method of computational analysis for cavitation process in TFP using the ANSYS CFX11 software [2]. Analyses were conducted for the TFP containing a half-open type impeller with 10 flat radial blades installed with tilt angle of 90 degrees. The basic pump parameters are: capacity $Q = 80\text{m}^3/\text{h}$, head $H = 20\text{m}$.

Calculation area consists of two following elements: the free chamber (FC), which is a stator element, and the impeller (IM), which is a rotating element. For each element of the work area, an unstructured calculation mesh was built. To simulate the flow in the boundary layer with sufficient accuracy, a layer, consisting of prismatic cells, was selected near the solid walls. There is a tetrahedral mesh for the FC and for the IM in the flow core area. The total number of elements of the computational mesh is 2 million 700 thousand cells. Flow simulation was realized in stationary definition.

At the initial stage, the calculation of flow was performed with conditions that eliminate cavitation occurrence. This calculation was performed for single-phase fluid using the standard $k - \epsilon$ turbulence model. Two interfaces were given in the work area between the stator and rotor elements: at the inlet to the IM and at the outlet from it. The "frozen rotor" data type of interfaces was accepted, which assumes averaging the parameters over time. As boundary conditions, there were specified mass flow rate at the inlet to the calculation area and the value of static pressure at the outlet. Flow calculation with the model of cavitation was the next stage. The boundary conditions had been changed: there were specified static pressure at the inlet and mass flow rate at the outlet. The calculation was carried out in a certain range of static pressures. Each subsequent calculation was carried out with a lower static pressure at the inlet by the accepted interval. Data from the cavitation free mode calculation had been used as an initial approximation for the first point, and then from the previous ones for each of the next point. It made possible to obtain the stalling cavitation characteristic at a constant flow rate.

3. Analysis of simulation results

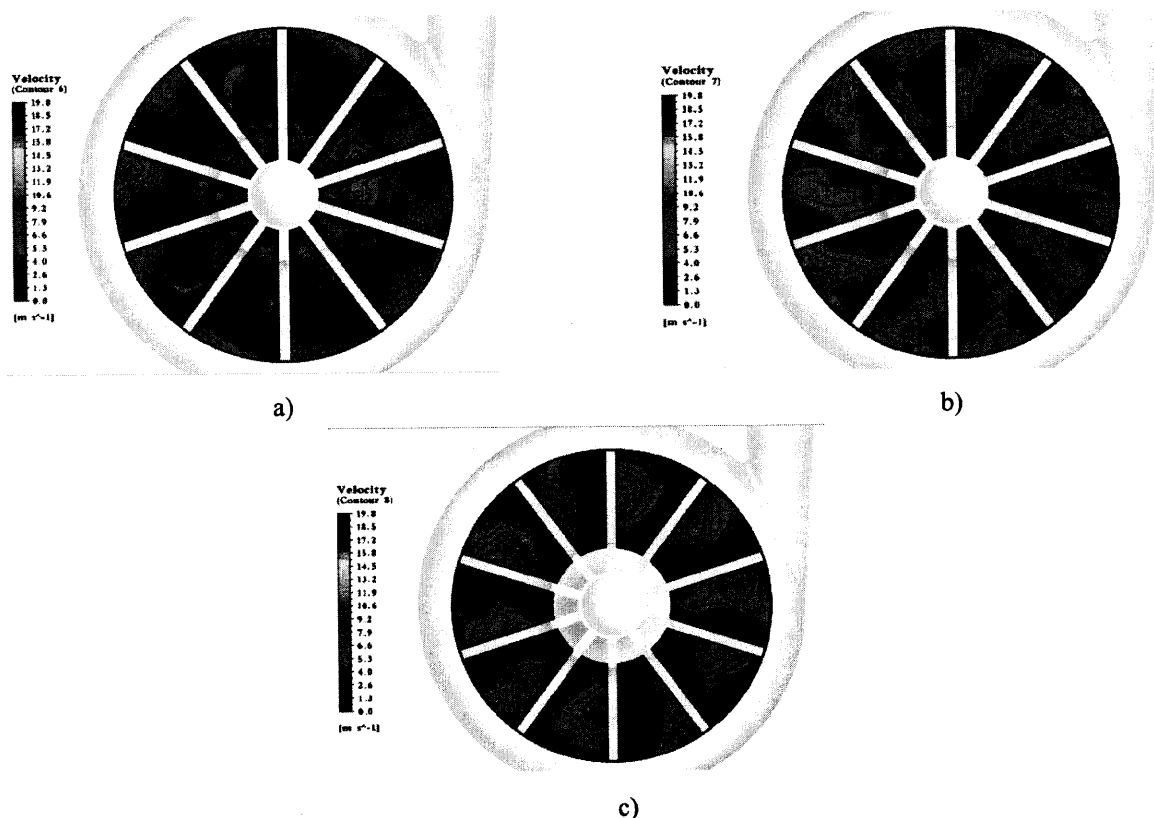
As a result of the flow structure analysis in the TFP setting at the cavitation free operation mode of the pump, distribution of absolute velocity and pressure had been obtained. Fig. 2 shows results of the calculation analysis of absolute velocity and pressure distribution nature in the pump IM between blades channels near the bushing and on the periphery. Velocity value (Fig. 2a) at the back side of the blade is higher than one at the work side, but the peripheral velocity is reduced to 0. At the back side of the blade, pressure value is less than one at the work side, but in the direction of IM outlet, pressure increases up to its largest values.

For more detailed understanding of nature of the fluid motion in the TFP impeller, calculations were performed in the IM sections (Fig. 3) in XY plane: on edges of the IM blades, at a distance of 22 mm from the IM inlet and near the basic disk.

On the section of the IM blades edges (Fig. 3a), areas of small velocities are located randomly, and at the periphery, velocities increase on the perimeter of the cylindrical niche. Nearby the bushing (Fig. 3b) along the fluid flow, areas of small absolute velocities increase; however, distribution of velocities in the between blades channels has approximately the same nature. (Fig. 3c) shows distribution of absolute velocity near the impeller basic disk. In this case, it becomes noticeable an expansion of small velocity area along the entire blade at its work side and high velocity area at the back side.



a) b)
Fig. 2 Distribution of absolute velocity and pressure in the between blades channels of the pump impeller



a) b) c)
Fig. 3 Distribution of absolute velocities in the IM sections

To explain the results, let us consider the work process of a TFP pump [3].

The fluid from the suction pipe enters into the impeller at the bushing area and is directed to the periphery under centrifugal force. Total flow of fluid in the pump consists of a flow in the FC and a flow in the IM. When the fluid flow goes out from the IM, one its part with a high reserve of energy goes to the outlet, and the second part loses energy reserve during interaction with the stream flow in the FC and is directed towards the inlet. As a result, fluid meridional motion or longitudinal vortex appears. Uneven distribution of velocities in longitudinal vortex affects the pressure value in the FC and IM. The mentioned fact is a cause of the uneven distribution of absolute velocity in the IM between blades channels along the direction of the fluid motion.

The presence of area of absolute velocity small values at the bushing area is explained by the presence of vortex area due to detached flow of the IM entrance edges or fluid flow inlet on a larger diameter.

Fig. 4 shows nature of absolute velocity change in the FC of the pump. For both IM and FC, the highest values of velocities are seen at the periphery of the setting. At the perimeter of the FC, uneven distribution of velocities takes place. With this, areas of high velocities are located symmetrically. The mentioned fact can be explained by deformation of the longitudinal vortex caused by influence of the pump outlet.

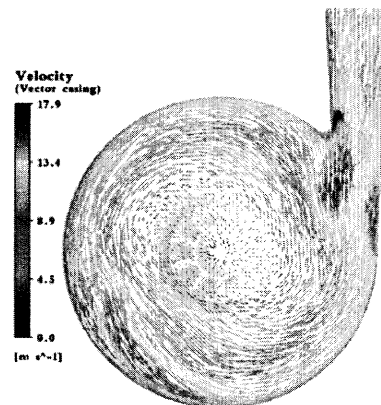


Fig. 4 Distribution of absolute velocity in the FC

Primary goal of the analysis was to calculate two-phase fluid with the cavitation model. As the initial data, results of the single-phase fluid calculation were used.

Investigation of cavitation phenomena and development of measures to prevent cavitation or to reduce its consequences are the part of the overall trends to energy and resource saving in the development and operation of pumping equipment. Cavitation should be considered as a major negative consequence, which prevents normal pump operation. To improve the design of pumps, it should be known locations of cavitation occurrence and causes of their onset.

As a result of the calculation, areas of cavitation onset and development in the TFP setting at various values of suction head have been determined, and a stalling cavitation characteristic has been obtained.

Result of the numerical calculation is confirmed by the physical experiment conducted earlier. Along with visual observations, photography of cavitation areas at different stages of its development was carried out (Fig. 5-10).

When suction head is $NPSH = 8.2$ m, on the back of the blade near the IM bushing, cavitation bubbles are visible (Fig. 5).

Formation of the cavitation area is explained by local pressure drop due to imperfect flow around the entrance edges. Though, bubbles aggregation areas do not form a continuous cavitation area. Bubbles periodically tear off from the blade surface and disappear in the IM between blades channels. Bubble size depends on the concentration of saturated steam fluid.

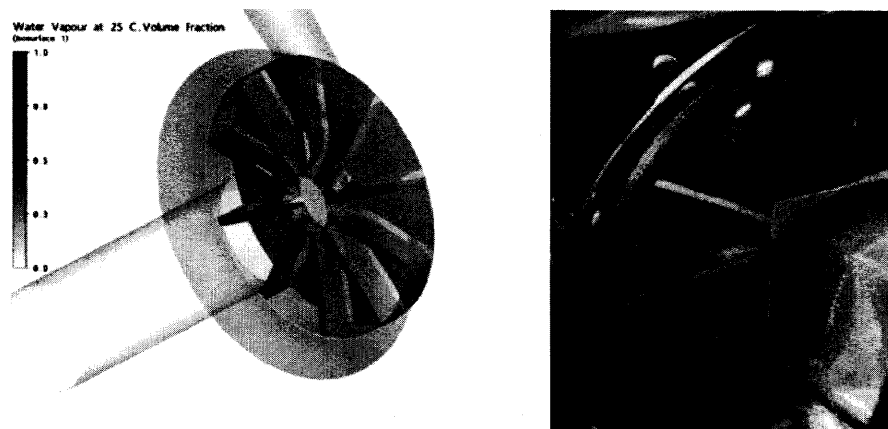


Fig 5. Cavitation areas when $NPSH = 8$ m

When suction head is $NPSH = 6.3$ m, cavitation bubbles have a clearer form. Aggregations of cavitation bubbles form a continuous cavitation area extending along the back side of the blade (Fig. 6). With this, pump head is practically unchanged.

When $NPSH = 4$ m, a border is clearly visible at the IM inlet in the minimum pressure area, downstream from which, at the rear side of the IM blade, cavitation bubbles move. Some of them fall into the between blades channels, and the other part goes to FC. It is distinguished by the gap cavitation appearing in the clearances between the ends of the blades on the outer diameter and the pump case cylindrical boring (Fig. 7).

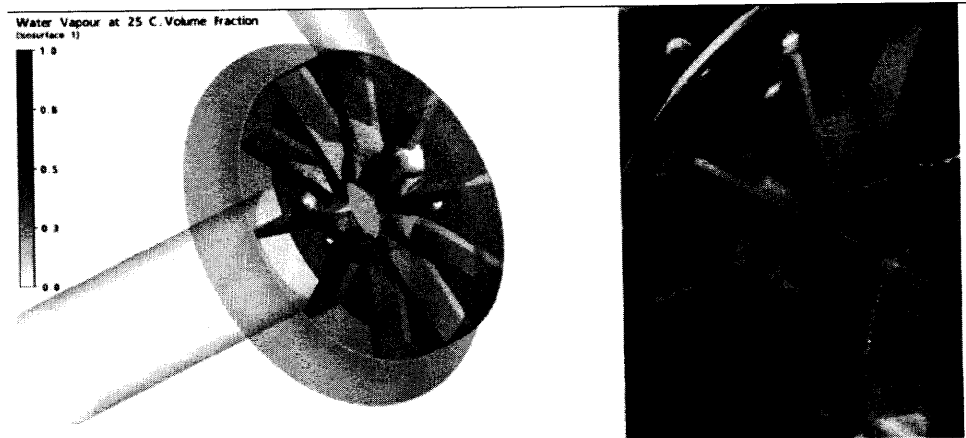


Fig 6. Cavitation areas when $NPSH = 6.3$ m

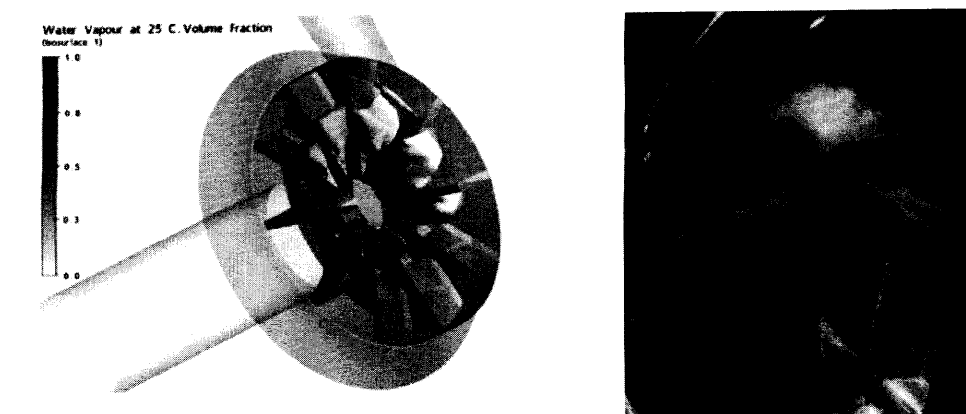


Fig 7. Cavitation areas when $NPSH = 4$ m

With further decreasing pressure on the pump inlet, when $NPSH = 3.7$ m, area of cavitation at the IM inlet is extended downstream (Fig. 8). Under these conditions, resistance of flow, running on the IM blades, increases. Effective cross-section of the active flow decreases, and velocity in the between blades channels increases. Vapor-liquid bubbles, having torn from the cavity, reach the IM outlet. This causes changing the flow parameters and consequently reducing the pump head.

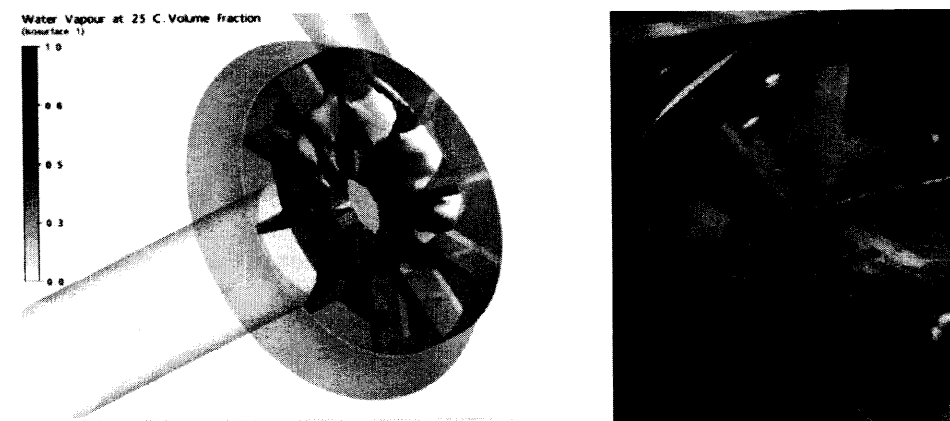


Fig 8. Cavitation areas when $NPSH = 3.7$ m

When suction head is $NPSH = 3.1$ m, demonstration of the cavitation areas intensify (Fig. 9). Stable cavitation area extends from the IM to the FC of the pump. The between blades channels are filled with a liquid-vapor mixture. Transfer of energy from the IM to fluid flow takes place at the peripheral area of the IM blades. Gap cavitation increases in size and spreads from the cylindrical niche to the FC. The pump head decreases, but does not drop sharply.

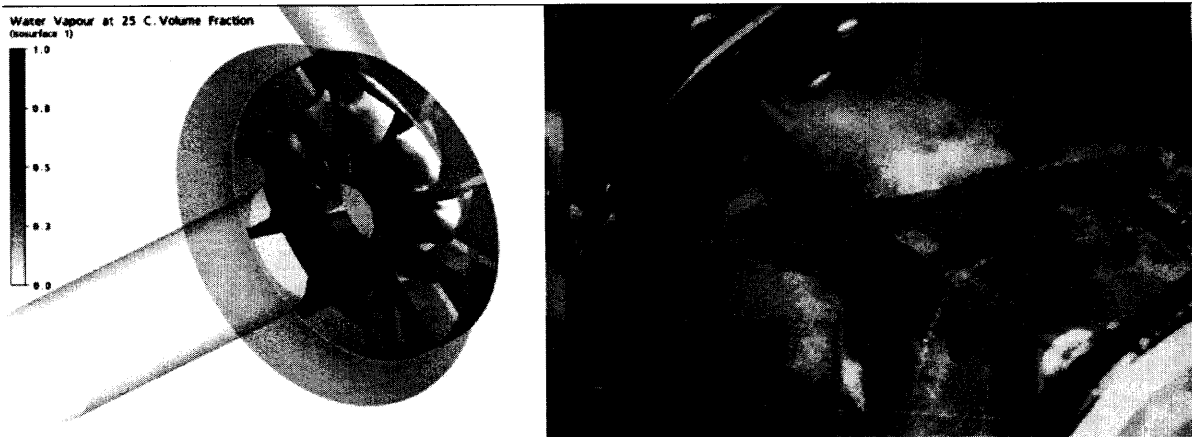


Fig 9. Cavitation areas when $NPSH = 3.1$ m

At the point 6, suction head is $NPSH = 1$ m. This case is characterized by increasing demonstration of the specified cavitation areas (Fig. 10). Cavitation area is almost completely filled the between blades channel, but fluid pumping continues.

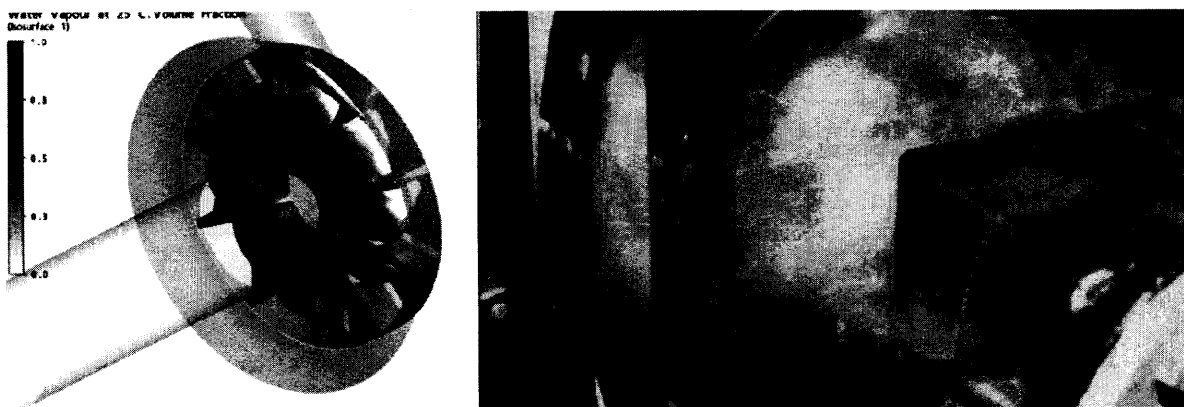


Fig 10. Cavitation areas when $NPSH = 1.5$ m.

When the pump inlet pressure decreases, the pump parameters change due to cavitation onset and development. Stall of the pump parameters takes place when cavitation is considerably developed.

Depending on the stage of cavitation development, radius of flow inlet to the impeller is changed. When the area of low pressure increases, power is transferred to flow by parts of the impeller blades in which pressure is higher than the pressure of saturated steam.

When the saturated steam pressure has been distributed throughout the between blades channel, stall of the pump parameters takes place. Cavitation occurrences in other locations (in the connection area of the inlet fitting with the free chamber of the pump, in the area of the outlet tongue, and gap cavitation at the impeller outlet) do not have an appreciable effect on the parameters stall, and hence on the suction capacity of the pump. Their influence appears only as an effect of such cavitation hazards as noise, vibration and cavitation erosion of the pump setting elements.

Fig. 11 a shows distribution of absolute velocity in the FC and IM of the pump during cavitation appearance. Virtually, initial cavitation does not have an effect on the nature of absolute velocity distribution in the IM and FC.

Fig. 11 b shows distribution of absolute velocity in the FC and IM of the torque flow pump, before the 3% drop of the pump head.

Fig. 11 c shows distribution of absolute velocity in the FC and IM of the torque flow pump after the 3% drop of the pump head; however the exchange of fluid energy takes place.

The results of analysis of the torque flow pump work process can represent an approximate pattern of fluid flow in

the free camera and in the impeller during cavitation onset and development. Areas of cavitation onset in the TFP have a certain place. Their location depends on many factors, which primarily include operating modes and conditions of fluid intake, and also the ratios of geometric dimensions of the pump setting [1].

Analyzing the obtained distribution of absolute velocity and pressure in the impeller between blades channels, we can conclude that cavitation in the TFP starts from the back side of the IM blade near the bushing. At the first stage of the process, compression of flow at the inlet to the IM takes place, resulting in increasing flow velocity and corresponding decreasing pressure. After the section has been compressed, flow expansion takes place: the kinetic energy falls, changing partly into the energy of pressure, and dissipates under the influence of dissipative forces. When cavitation area at the inlet to the IM expands, fluid flow from the inlet fitting goes to the between blades channels. The process of the flow compression and expansion is repeated. With pressure increasing after compression of the section, cavitation bubble collapse takes place in the IM between blades channels or in the FC.

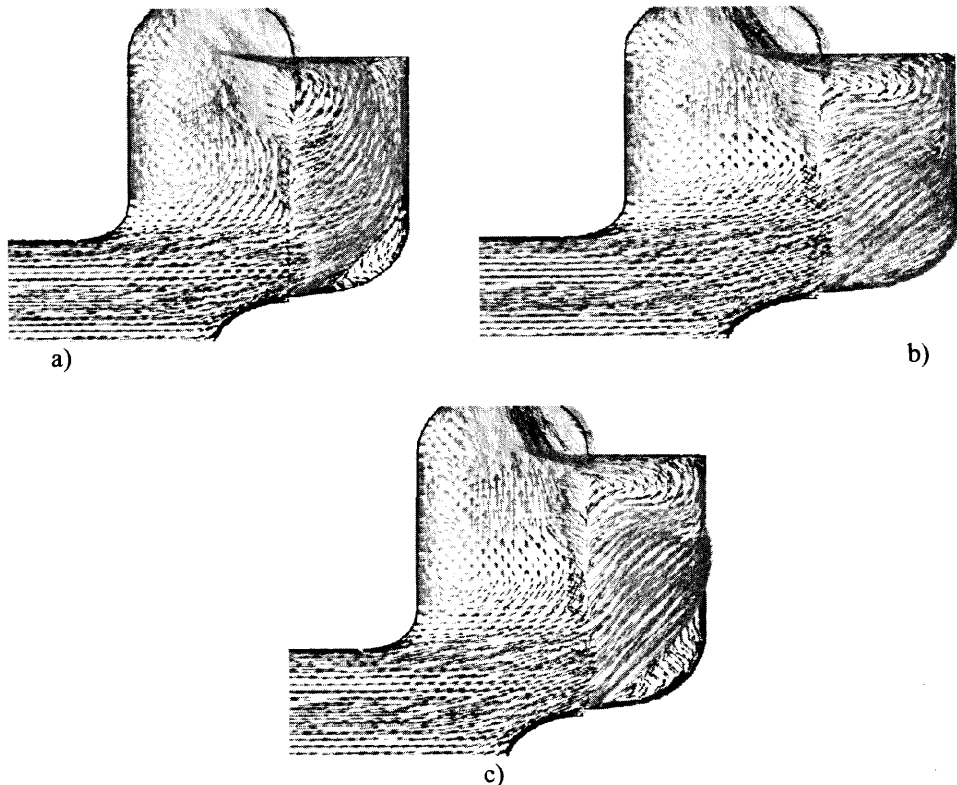


Fig. 11 - Distribution of absolute velocity in the IM and FC: a - appearance of cavitation, b - before the 3% drop of the pump head, c - developed cavitation.

According to the results of the numerical calculation, a stalling cavitation characteristic of the torque flow pump was built (Fig. 12).

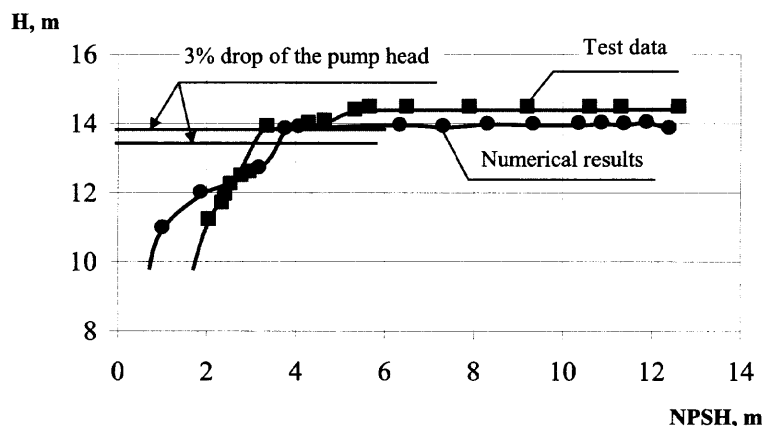


Fig. 12 - Stalling cavitation characteristic of the torque flow pump 3% drop of the pump head curve.

With decreasing pressure at the pump inlet, cavitation process in the setting starts before the stall of the pump operating mode takes place. After reaching a certain size of the cavitation area, the pump head decreases compared to its initial value, but a sharp drop does not happen. And only after spreading the cavitation area along the setting, the head gradually decreases. Sharp stall of the parameters does not take place in TFP, and this is their advantage in use.

4. Conclusions

Comparing results of the numerical calculation, we can draw some conclusions:

1. relationship between a pattern of the fluid flow and cavitation onset start and development has been obtained;
2. cavitation arises in the IM at the back side of the blade near the bushing;;
3. areas of cavitation onset in the Turo type TFP with the IM have been determined;
4. cavitation in the TFP exists long before the stall of its parameters;
5. sizes of the cavities are not completely identical in all between blades channels due to their different location relative to the pump outlet;
6. stall of the pump operation is a consequence of cavitation expansion along width of the between blades channels and spread of cavitation bubbles in the free camera.

Nomenclature

H	head [m]
Q	capacity [m^3/h]
$NPSH$	net positive suction head [m]

References

- [1] Kotenko A.I., German V.F. Estimation of the cavitation characteristics of torque flow pumps // Bulletin of the Sumy State University, Sumy, 2008. No 2 (10), pp. 81-84.
- [2] ANSYS CFX-Solver, Theory Guide. Release 11. 2006. - 298 p.
- [3] German V.F. Investigation of flow structure in torque flow pump // "Hydraulic machines and hydropneumatic units: Theory, Solve, Design", Papers of Conference, Kiev, 1994, pp. 67-81.